Electronic Supplementary Material (ESI) for Dalton Transactions.

Supporting Information for

A Reagent for Heteroatom Borylation, Including Iron Mediated Reductive Deoxygenation of Nitrate to a Di-Nitrosyl Iron Complex

Daniel M. Beagan, Veronica Carta and Kenneth G. Caulton*

Table of Contents

Experimental

General. All reactions were carried out under an atmosphere of ultra-high purity gas using standard Schlenk techniques under Ar or in a glovebox under N_2. Solvents were purchased from commercial sources, purified using Innovative Technology SPS-400 PureSolv solvent system or by distilling from conventional drying agents and stored over activated 4 Å molecular sieves. Glassware was oven-dried at 170 °C overnight or flame dried prior to use. NMR spectra were recorded in various deuterated solvents at 25 °C on a Varian Inova -400 or 500 spectrometer (^{1}H: 400.11 MHz, 500.11 MHz, respectively). Chemical shifts are reported in ppm from tetramethylsilane or the residual solvent as an internal standard: integration multiplicity (s = singlet, d = doublet, t = triplet, m = multiplet, br = broad). All starting materials have been obtained from commercial sources and used as received without further purification. $(Bpin)_2Pz$ was synthesized via the established procedure using THF as the solvent.[1]

General procedure for the stoichiometric borylation of azobenzene

To a J-Young tube containing azobenzene (16 mg, 0.0875 mmol, 1 equiv.) in d_8-toluene was added **1** (29 mg, 0.0875 mmol, 1 equiv.) also dissolved in d_8-toluene. The resulting solution was allowed to heat in an oil bath at 110 °C for 36 hours, during which there was a color change from deep orange to yellow. ^{1}H NMR showed complete consumption of both starting materials after 36 hours of heating. The reported spectrum for borylated azobenzene[2] was done in C_6D_6; therefore, the completed reaction was brought into the glovebox, dried in vacuo, and redissolved in C_6D_6 for spectroscopic assay.

1,2-diphenyl-1,2-bis(4,4,5,5-tetramethyl-1,3,2dioxaborolan-2-yl)hydrazine: ^{1}H NMR (400 MHz, C_6D_6, 298K) δ(ppm) 7.68 (d, J_{H-H} = 8.0 Hz, 4H) 7.09 (t, J_{H-H} = 7.4 Hz, 4H) 6.75 (t, J_{H-H} = 7.1 Hz, 2H) 1.06 (s, 12H) 1.02 (s, 12H).

Catalytic borylation of azobenzene

To a J-Young tube containing azobenzene (16 mg, 0.0875 mmol, 1 equiv.) in d_8-toluene was added $(Bpin)_2$ (22 mg, 0.0875 mmol, 1 equiv.) in d_8-toluene and 4,4'-bipyridine (4.1 mg, 0.026 mmol, 0.3 equiv.) also dissolved in d_8-toluene. The resulting solution was allowed to heat in an oil bath at 110 °C for 12 hours, during which the color changed from orange to yellow and ^{1}H NMR showed complete consumption of $(Bpin)_2$ and azobenzene.

1,2-diphenyl-1,2-bis(4,4,5,5-tetramethyl-1,3,2dioxaborolan-2-yl)hydrazine: ^{1}H NMR (400 MHz, d_8-toluene, 298K) δ(ppm) 7.68 (d, J_{H-H} = 8.2 Hz, 4H) 7.17 (t, J_{H-H} = 7.8 Hz, 4H) 6.83 (t, J_{H-H} = 7.5 Hz, 2H) 1.18 (s, 12H) 1.13 (s, 12H). ^{13}C NMR (126 MHz, d_8-toluene, 298K) δ(ppm) 146.15, 121.12, 120.79, 116.62, 83.11, 24.43, 24.03.

Catalytic borylation of Benzo(c)cinnoline, bcc

To a J-Young tube containing bcc (18 mg, 0.10 mmol, 1 equiv.) dissolved in C_6D_6 was added $(Bpin)_2$ (25.4 mg, 0.10 mmol, 1 equiv.) in C_6D_6 and 4,4'-bipyridine (4.7 mg, 0.03 mmol, 0.3 equiv.) also dissolved in C_6D_6. The resulting yellow solution was allowed to heat in an oil bath at 100 °C and the reaction was monitored by ^{1}H NMR spectroscopy. The bcc was completely consumed after 40 hours of heating, to afford a deep yellow solution.

2,2'-biphenyl-1,1'-bis(4,4,5,5-tetramethyl-1,3,2dioxaborolan-2-yl)hydrazine: ^{1}H NMR (400 MHz, C_6D_6, 298K) δ(ppm) 7.67 (d, $J_{H,H}$ = 8.8 Hz, 2H), 7.38 (d, $J_{H,H}$ = 8.7 Hz, 2H), 6.99 (t, $J_{H,H}$ = 7.7 Hz, 2H), 6.81 (t, $J_{H,H}$ = 9.0 Hz, 2H), 1.03 (s, br, 24 H).

Borylation competition between azobenzene and Benzo(c)cinnoline

To a J-Young tube containing azobenzene (20 mg, 0.110 mmol, 1 equiv.) and bcc (19.8 mg, 0.110 mmol, 1 equiv.) dissolved in d_8-toluene was added $(Bpin)_2$ (27.9 mg, 0.110 mmol, 1 equiv.) and 4,4'-bipyridine (5.1 mg, 0.03 mmol, 0.3 equiv.) also dissolved in d_8-toluene and the solution was heated in an oil bath at 110 °C. The orange solution was monitored periodically by ^{1}H NMR, and after 40 hours of heating there was consumption of all $(Bpin)_2$. The ^{1}H NMR shows that the main product formed is borylated bcc, with small amounts of borylated azobenzene seen in the methyl region but almost undetectable amounts in the aromatic region.

Borylation of $TMSN_3$

To a J-Young tube containing $TMSN_3$ (12 mg, 0.104 mmol, 1 equiv) in C_6D_6 was added $(Bpin)_2$ (26.4 mg, 0.104 mmol, 1 equiv) and 4,4'-bipyridine (4.9 mg, 0.104 mmol, 0.3 equiv.). The resulting solution was heated in an oil bath at 100 °C for 12 hours, after which ^{1}H NMR shows complete consumption of $TMSN_3$.

Trimethylsilyl-bis(4,4,5,5-tetramethyl-1,3,2dioxaborolan-2-yl) amine: ^{1}H NMR (400 MHz, C_6D_6, 298K) δ(ppm): 1.02 and 0.99 (2s, 24H) 0.15 (s, 9H)

Borylation of Ph_2Tz

To a J-young tube containing Ph_2Tz (20 mg, 0.064 mmol, 1 equiv.) in d_8-THF was added $(Bpin)_2$ (16.3 mg, 0.064 mmol, 1 equiv.) and 4,4'-bipyridine (3.0 mg, 0.02 mmol, 0.3 equiv.) and the solution was heated to 80 °C. The pink solution slowly changed to a red, then a yellow solution, and after 12 hours of heating all $(Bpin)_2$ was consumed.

3,6-diphenyl-1,4-bis(4,4,5,5-tetramethyl-1,3,2dioxaborolan-2-yl) tetrazine: ^{1}H NMR (400 MHz, d_8-THF , 298K) δ(ppm): 7.57 (d, $J_{H,H}$ = 7.7 Hz, 4H) 7.36 (t, $J_{H,H}$ = 7.2 Hz, 2H) 7.29 (t, $J_{H,H}$ = 7.5 Hz, 4H) 1.15 (s, 24H). ^{13}C NMR (126 MHz, d_8-toluene, 298K) δ(ppm) 155.14, 132.80, 129.71, 129.12, 83.22, 24.12.

General procedure for the deoxygenation of nitrobenzene

To a J-young tube containing nitrobenzene (10 mg, 0.08 mmol) in C_6D_6 was added $(Bpin)_2$bpy (81.8 mg, 0.2 mmol) as a slurry in C_6D_6. The heterogeneous solution was allowed to mix on an NMR spinner for 30 minutes, and as the $(Bpin)_2$bpy reacted, the yellow solution became homogeneous. ^{1}H NMR assay after 30 minutes showed complete consumption of $(Bpin)_2$bpy as well as $PhNO_2$. When this reaction is done instead with $(Bpin)_2$Pz, there is less than 50% conversion to the desired product, with a variety of other unidentified products being formed.

N,O-bis(4,4,5,5-tetramethyl-1,3,2dioxaborolan-2-yl)phenylhydroxylamine: ^{1}H NMR (400 MHz, C_6D_6, 298K) δ(ppm): 7.56 (d, $J_{H,H}$ = 8.1 Hz, 2H) 7.10 (t, $J_{H,H}$ = 7.9 Hz, 2H) 6.71 (t, $J_{H,H}$ = 7.3 Hz, 1H) 1.04 (s, 12H) 1.00 (s, 12H).

Synthesis of (DIM)FeCl$_2$. The established procedure for the synthesis of other (α-diimine)FeCl$_2$ complexes was followed. To a stirring solution of $FeCl_2$ as a slurry in THF was added dropwise DIM also dissolved in THF. There was a color change to dark blue upon the addition of DIM, and the resulting solution was allowed to stir for 12 hours, upon which there was a dark maroon precipitate. The blue solution was filtered through celite, and the solid washed with excess THF until the THF was colorless. Removal of the THF in vacuo gave a purple solid. ^1H NMR (400 MHz, CD_3CN, 298K) δ(ppm) 113.0 (br s, 4H) 15.1 (br s, 6H) 11.32 (br s, 12H) 3.7 (br s, 6H).

Synthesis of (DIM)Fe(NO$_3$)$_2$(MeCN) 4. To a stirring solution of DIMFeCl$_2$ (200 mg, 0.447 mmol) in MeCN was added $AgNO_3$ (152 mg, 0.895 mmol) also dissolved in MeCN dropwise, resulting in a slight color change to dark purple and the formation of a white precipitate. After filtration through celite to remove AgCl and removal of the solvent in vacuo, the purple solid was redissolved in a minimal amount of MeCN, and ether was added leading to the precipitation of the dark purple solid **4** (199 mg, 90% yield). ^1H NMR (400 MHz, CD_3CN, 298K) δ(ppm) 19.70 (br s, 6H) 14.85 (br s 4H) 14.08 (br s, 6H) 8.38 (br s 12H). IR ν_{NO}: 1506 and 1270 cm^{-1}.

Synthesis of (DIM)Fe(NO)$_2$ 5. To a J-Young tube containing **4** (30 mg, 0.06 mmol) dissolved in d_8-THF was added (Bpin)$_2$Pz (80.8 mg, 0.24 mmol) also dissolved in d_8-THF, resulting in a color change from yellow to dark purple. After heating at 80 °C for two hours, the reaction was complete. Removal of the solvent in vacuo and rinsing (3 x 5 mL) with cold pentane (-35 °C) gave the purple solid **5** (23 mg, 88% yield). ^1H NMR (400 MHz, d_8-THF, 298K) δ(ppm) 6.86 (s, 4H) 2.23 (s, 6H), 2.16 (s, 6H) 2.11 (s, 12 H). IR ν_{NO}: 1697 1645 cm^{-1}.

Oxidation of (DIM)Fe(NO)$_2$. To a J-Young tube containing **5** (25 mg, 0.06 mmol) dissolved in d_8-THF was added [Fe(Cp)$_2$](OTf) (19 mg, 0.06 mmol) also dissolved in d_8-THF. A slight color change was observed from dark purple to maroon, and after 30 minutes the ^1H NMR signals for **5** were absent. This solution was then transferred to an EPR tube for data collection.

1. K. Oshima, T. Ohmura and M. Suginome, *Chem. Commun.*, 2012, **48**, 8571-8573.
2. M. B. Ansell, G. E. Kostakis, H. Braunschweig, O. Navarro and J. Spencer, *Adv. Synth. Catal.*, 2016, **358**, 3765-3769.

Spectral Data

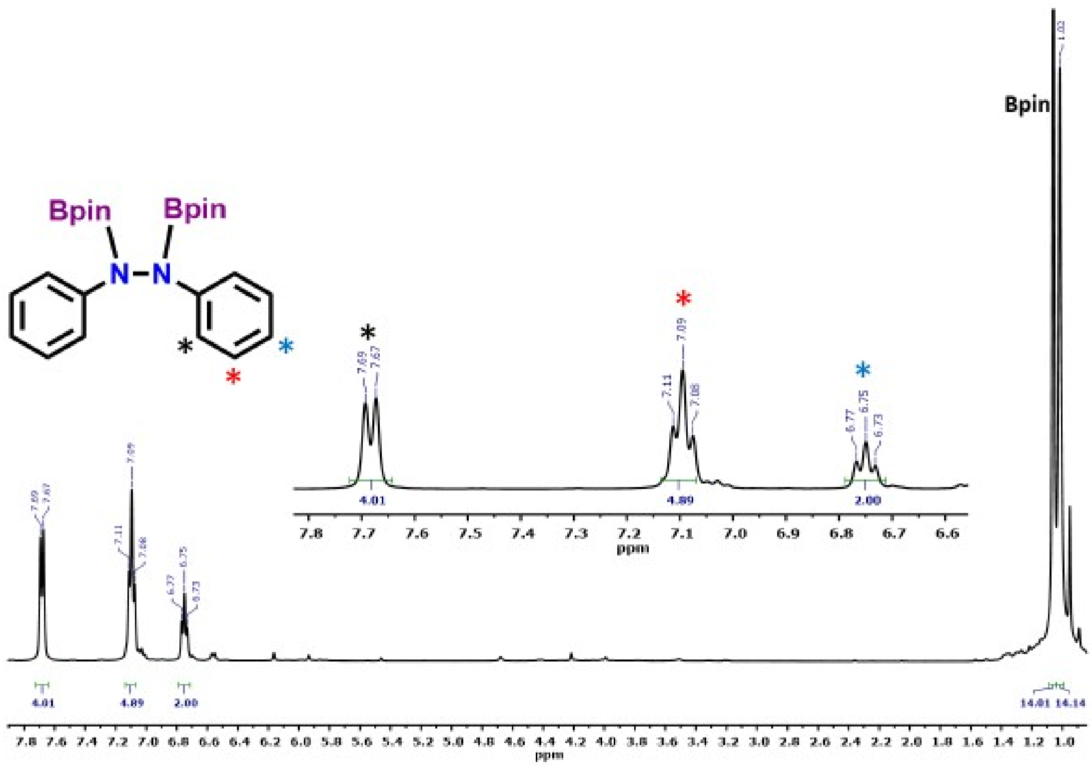

Figure S1. ^{1}H NMR spectrum of borylated azobenzene in C_6D_6

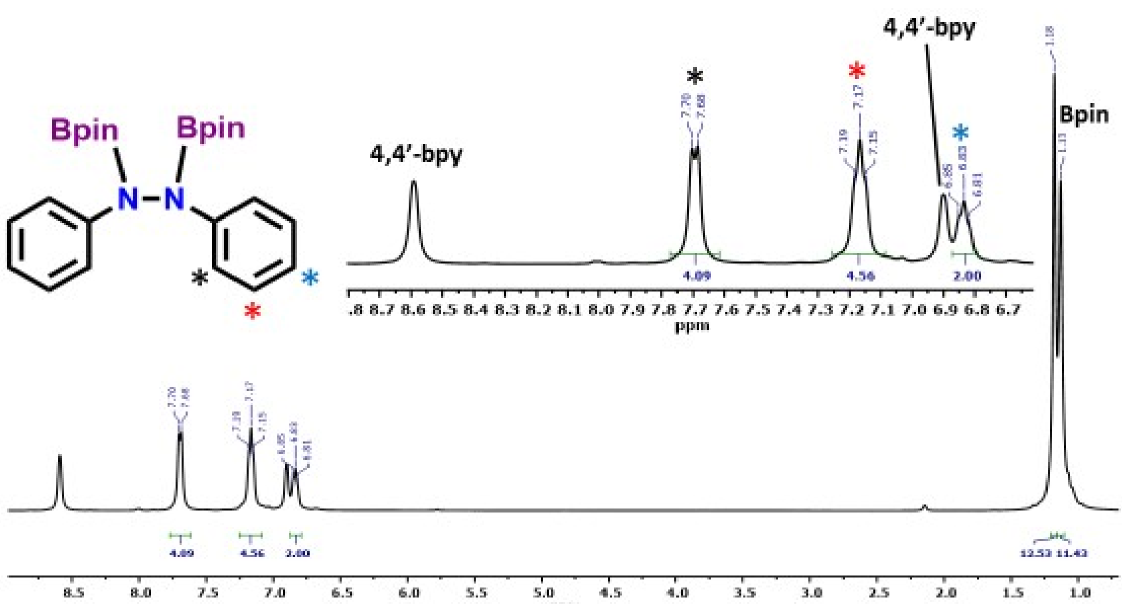

Figure S2. ^{1}H NMR spectrum of reaction between azobenzene, $(Bpin)_2$, and 4,4'-bpy in d_8-toluene

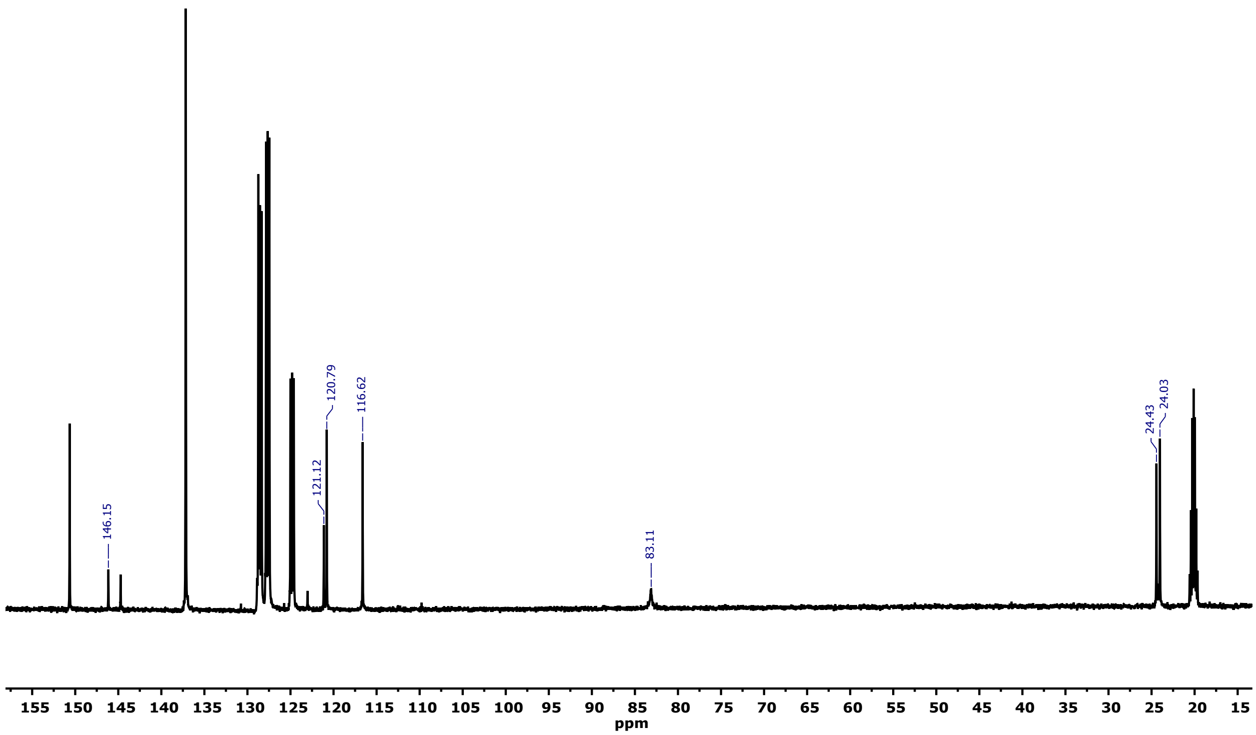

Figure S3. ^{13}C NMR in toluene of borylated azobenzene. Unlabeled peaks are 4,4'-bpy and toluene

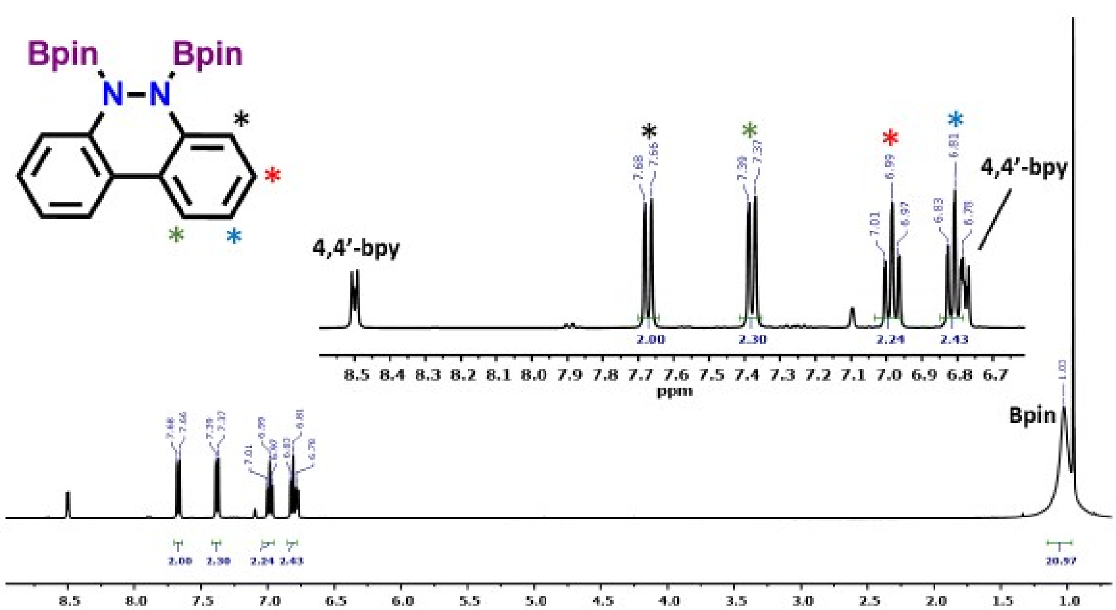

Figure S4. ^{1}H NMR spectrum of reaction between benzo-c-cinnoline, $(Bpin)_2$, and 4,4'-bpy in C_6D_6

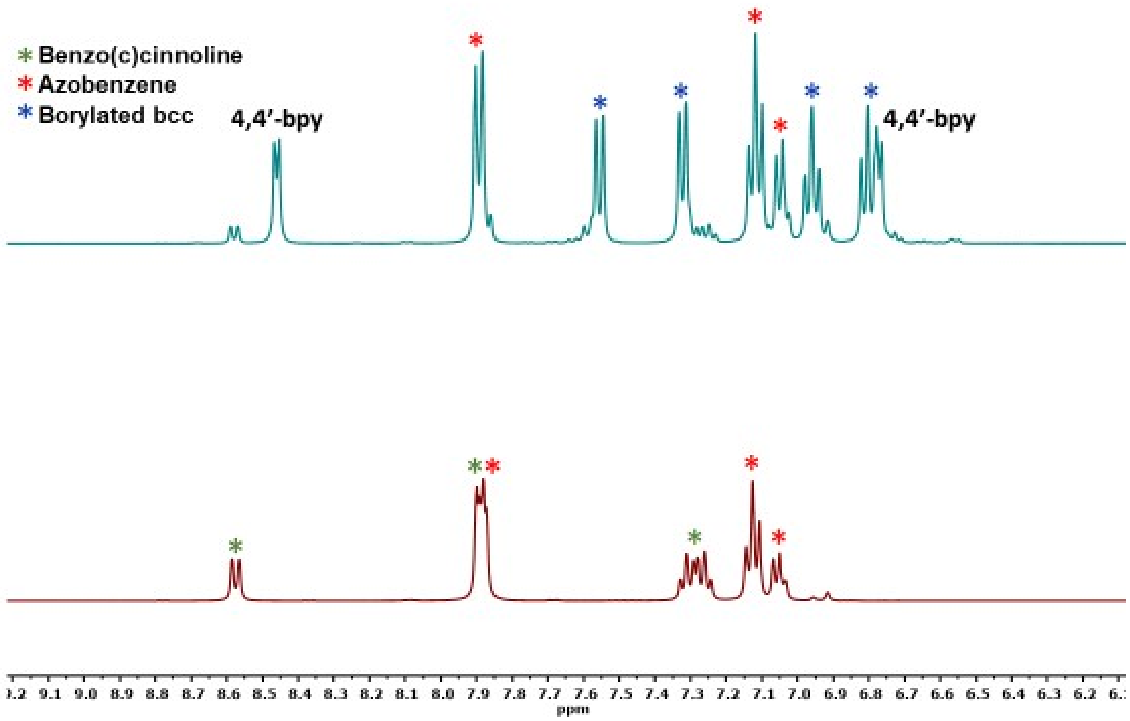

Figure S5 Aromatic region of ^{1}H NMR spectrum of benzo(c)cinnoline, azobenzene before addition of 4,4'-bpy (bottom) and after 20 hours of heating with 4,4'-bpy and $(Bpin)_2$ (top) showing almost complete consumption of bcc, formation of borylated bcc, and unreacted azobenzene.

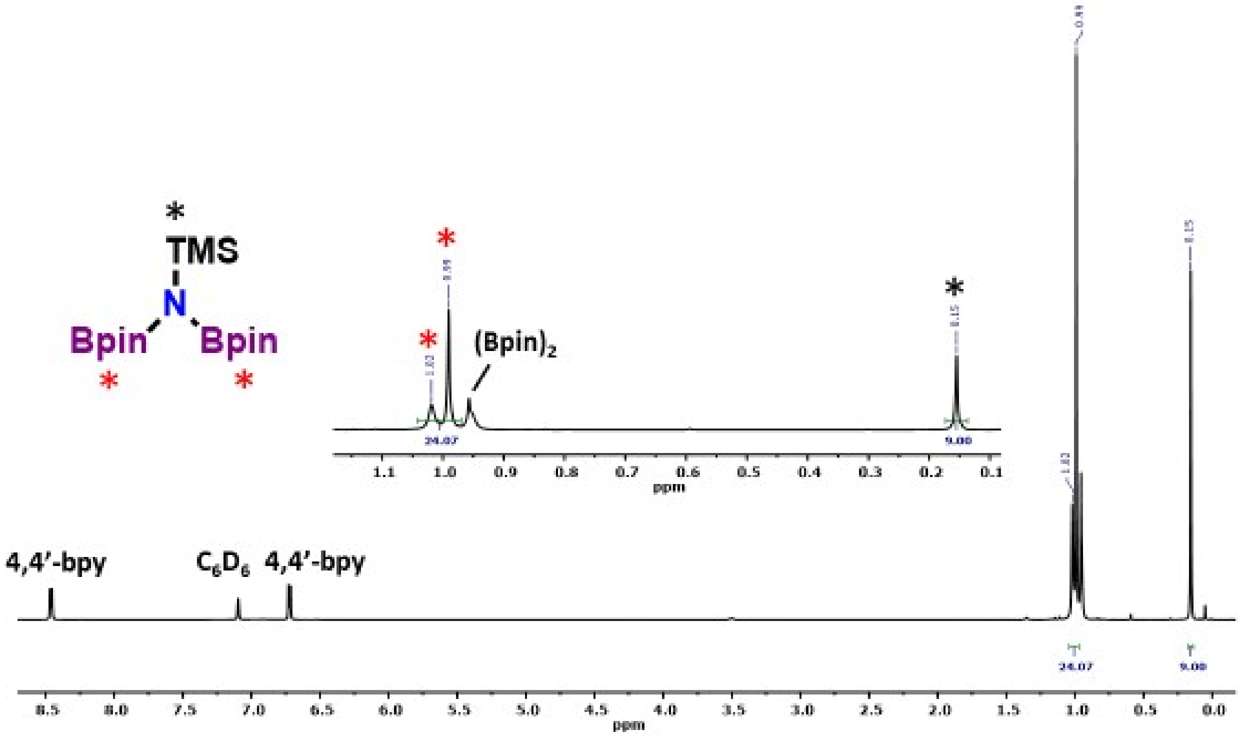

Figure S6. ^{1}H NMR spectrum of borylated amine in C_6D_6

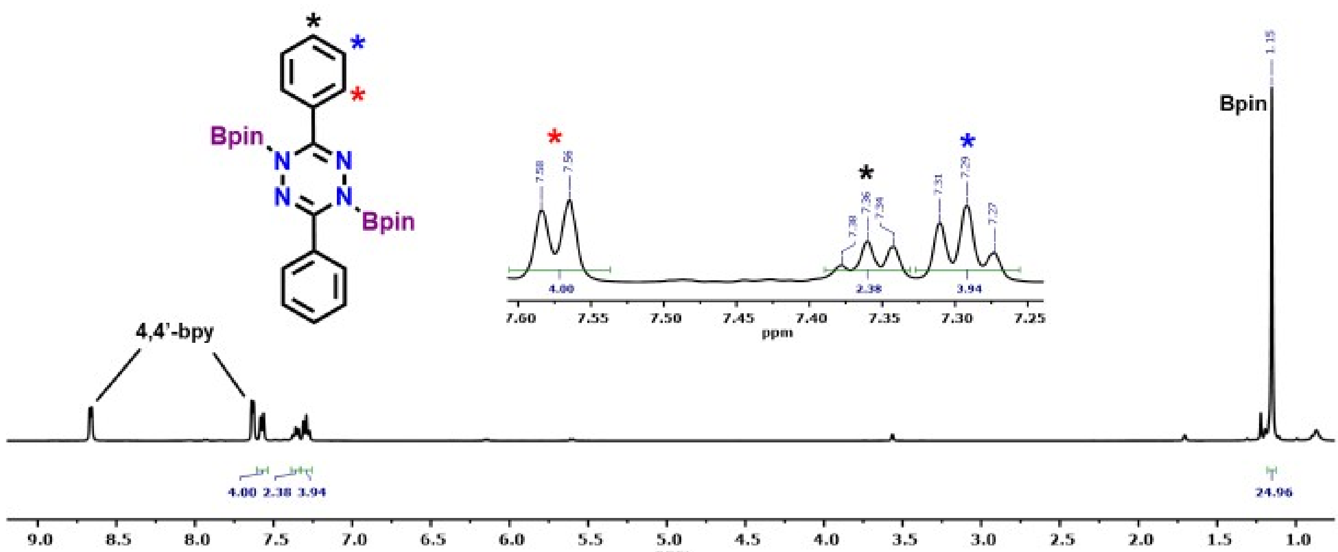

Figure S7. ^{1}H NMR spectrum of borylated Ph_2Tz in d_8-THF

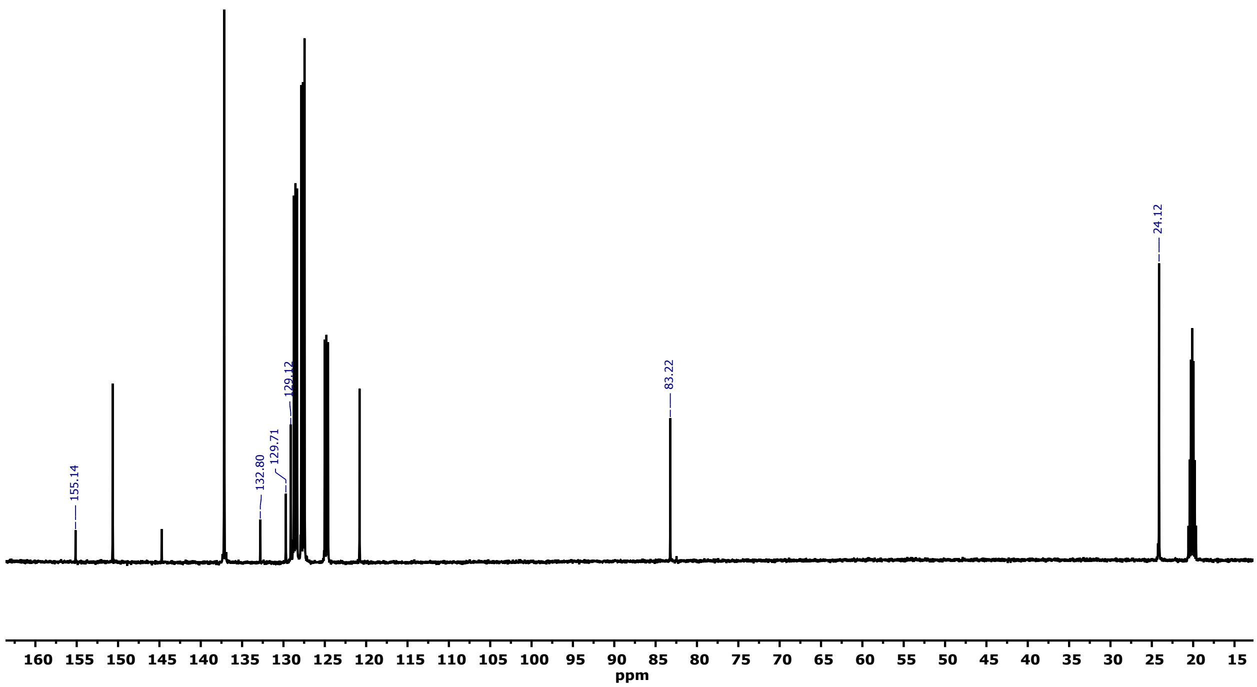

Figure S8. ^{13}C NMR in toluene of borylated diphenyl tetrazine. Unlabeled peaks are 4,4'-bpy and toluene

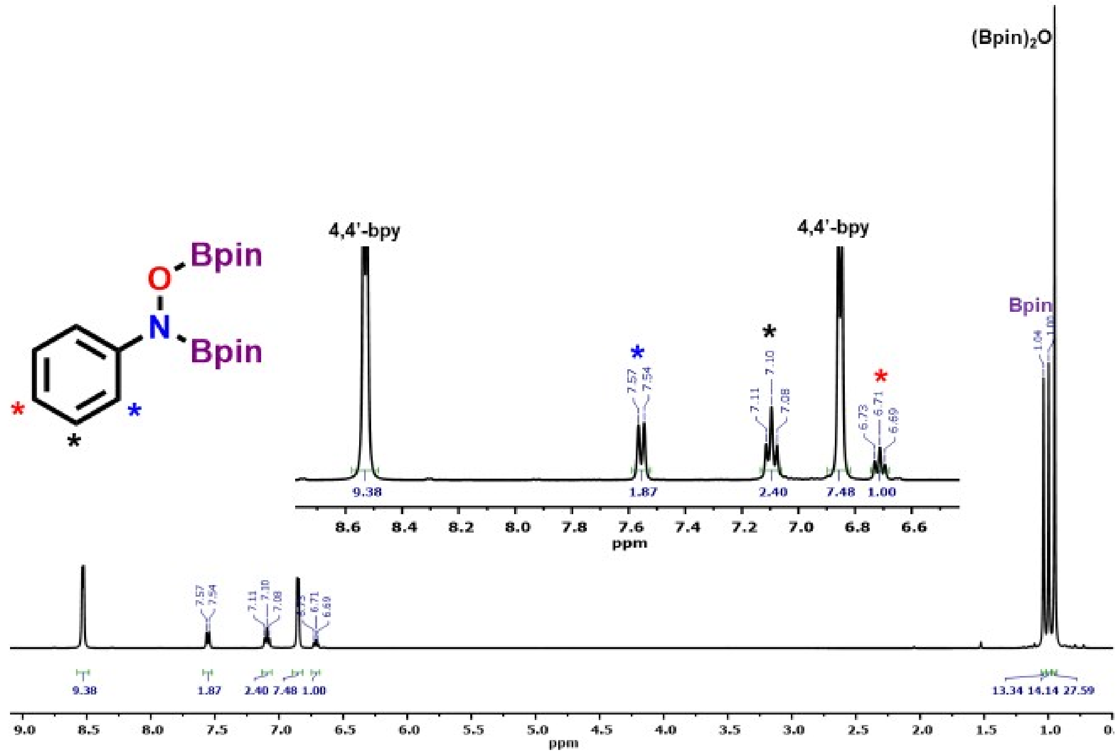

Figure S9. [1]H NMR spectrum of N/O borylated nitrosobenzene in C_6D_6

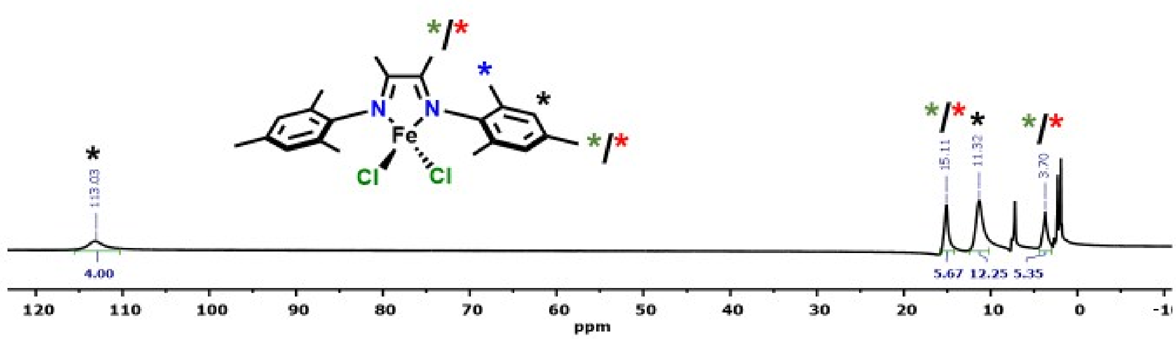

Figure S10. [1]H NMR spectrum of DIMFeCl_2 in CD_3CN. Unlabeled peaks are residual acetonitrile and toluene.

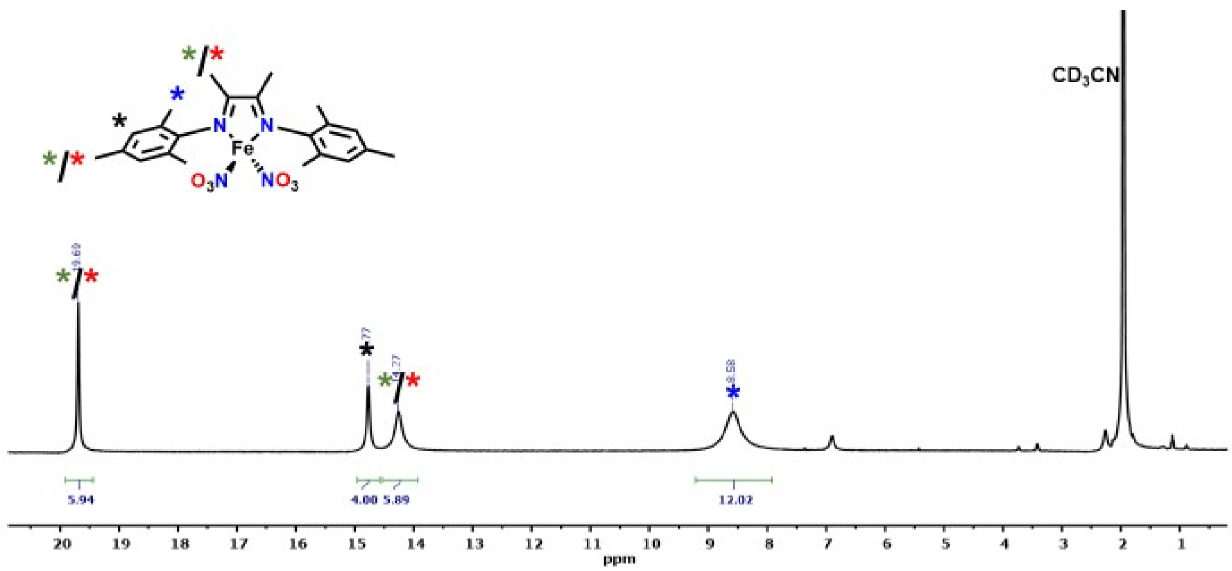

Figure S11. ^{1}H NMR spectrum of (DIM)Fe(NO_3)$_2$(MeCN) in CD_3CN

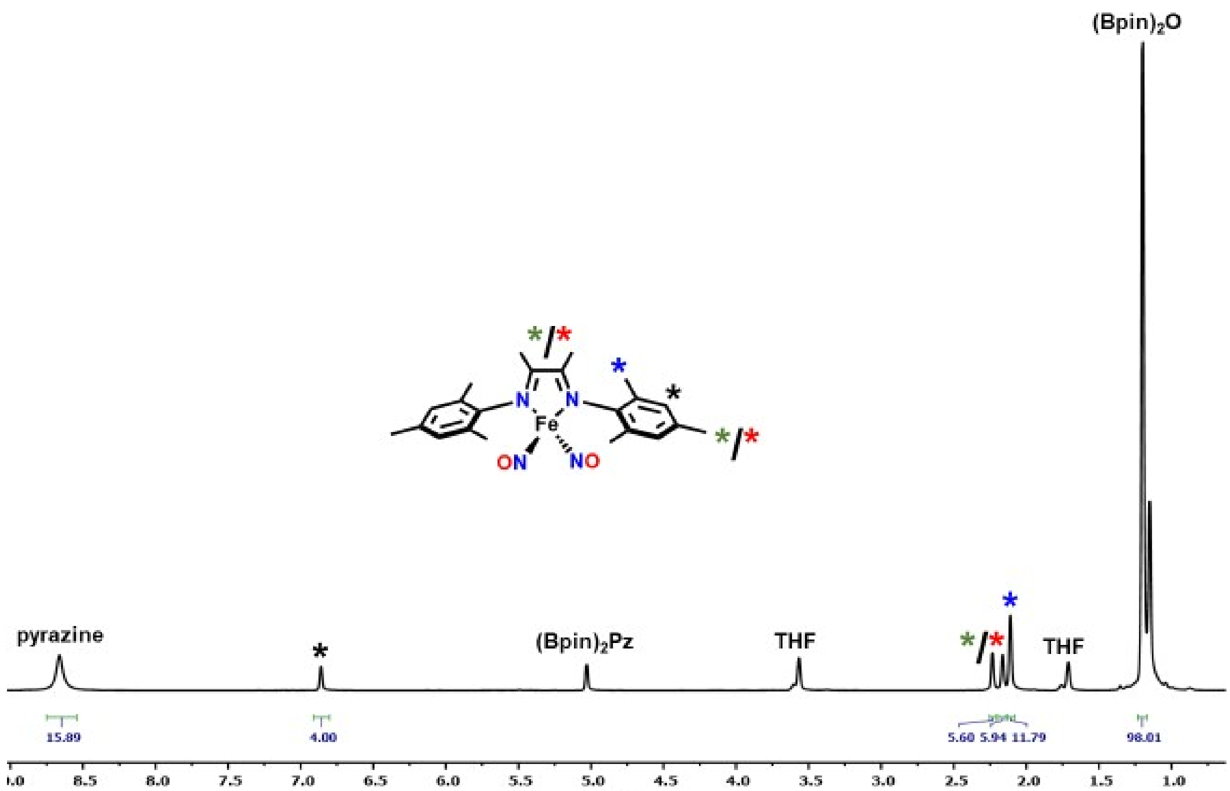

Figure S12. ^{1}H NMR spectrum of (DIM)Fe(NO)$_2$ in d_8-THF

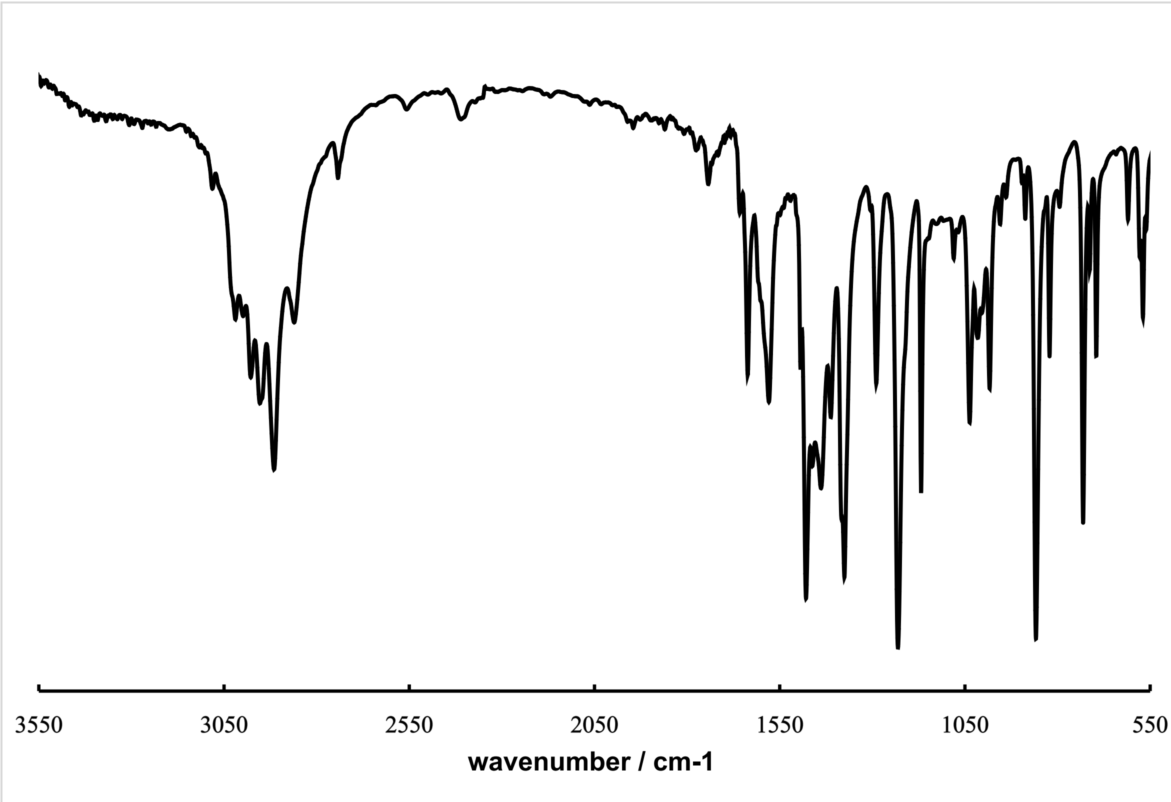

Figure S13. IR spectrum of (DIM)$FeCl_2$ (KBr press)

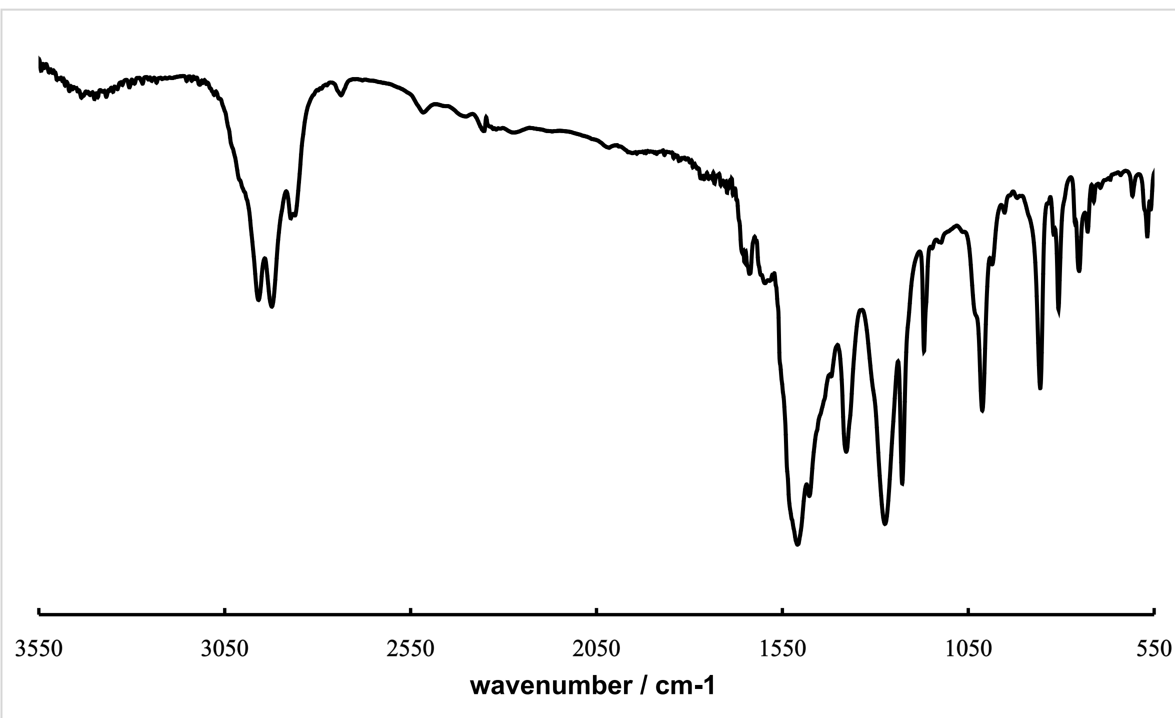

Figure S14. IR spectrum of (DIM)$Fe(NO_3)_2$(MeCN) (KBr press)

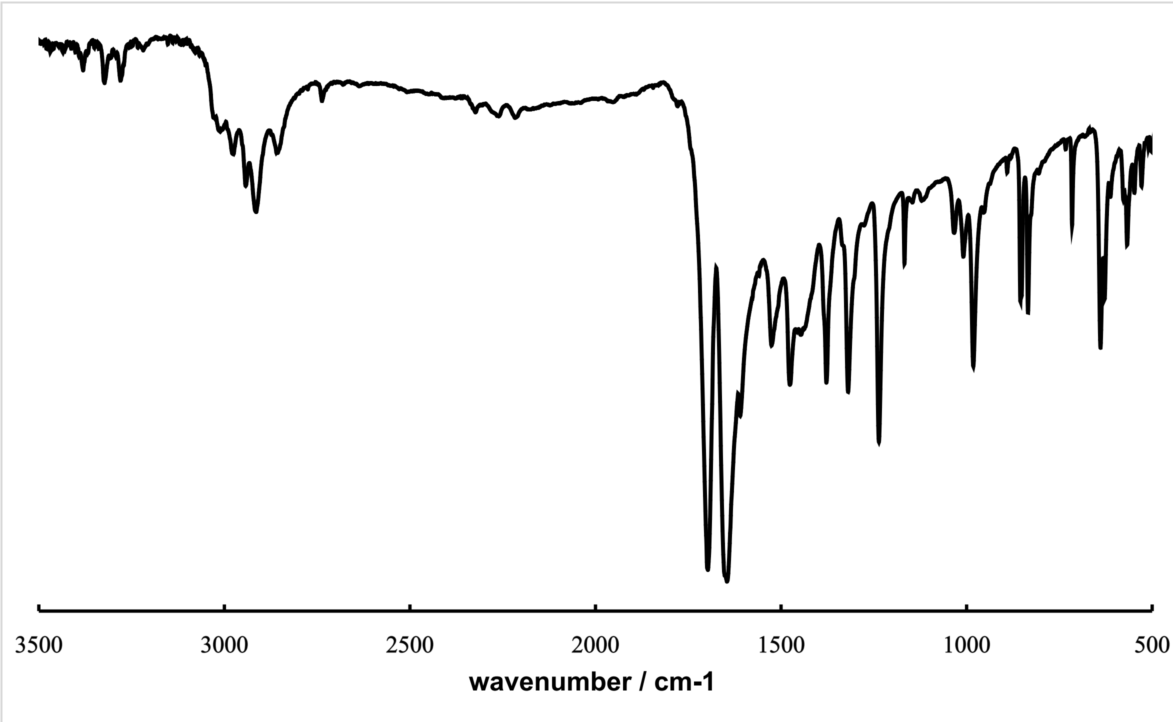

Figure S15. IR spectrum of $(DIM)Fe(NO)_2$ (KBr press)

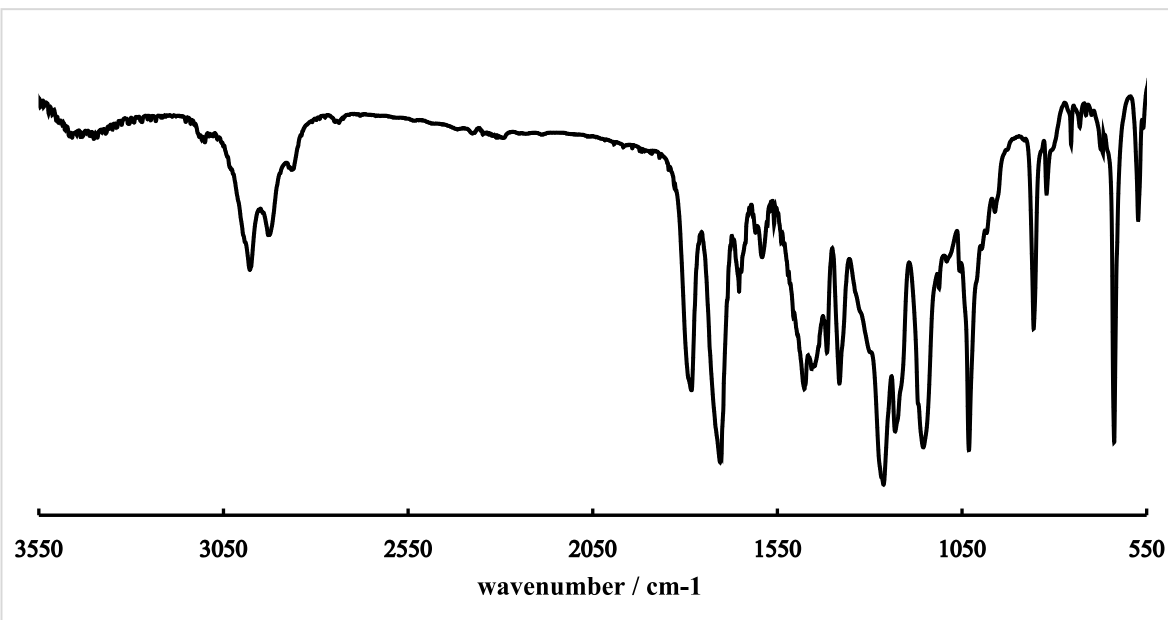

Figure S16. IR spectrum of $[(DIM)Fe(NO)_2]^+$

EPR Simulation

The experimental EPR spectrum was simulated using EasySpin[1] to obtain the coupling constants reported in this manuscript. As seen in Figure S15, despite relative intensities being different, the coupling constants match well. Attempts to model the spectrum with coupling to 3 nitrogens, 2 equivalent and 1 inequivalent, were unsuccessful.

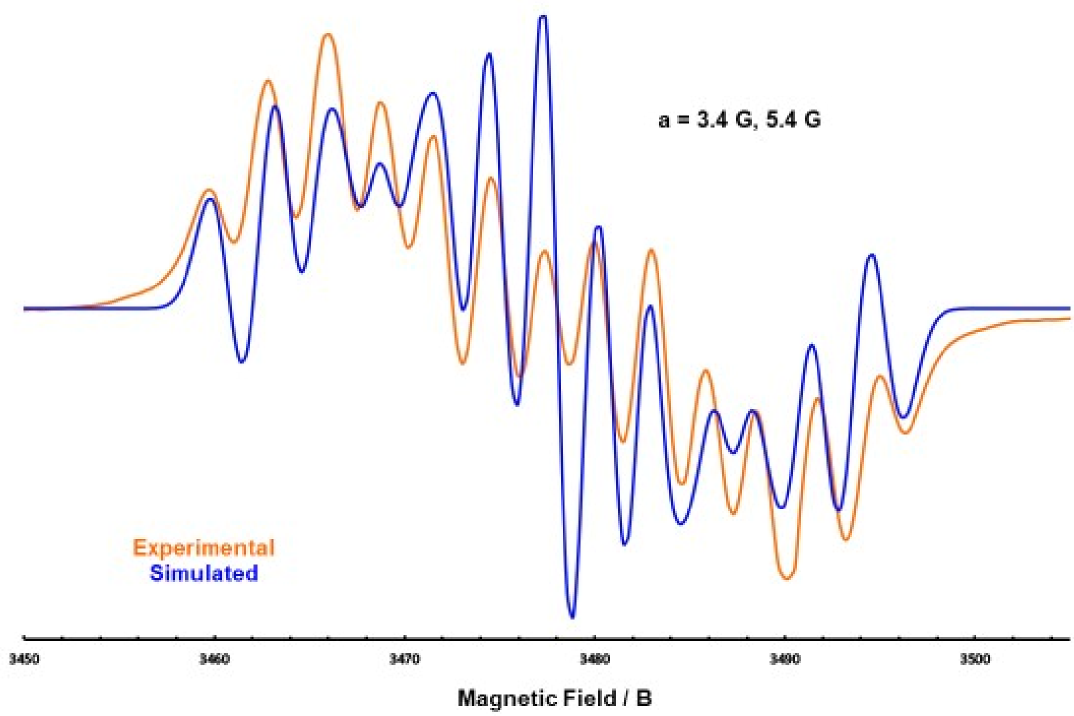

Figure S17. Simulated and experimental EPR spectra overlaid for $[(DIM)Fe(NO)_2]^+$

1. S. Stoll, A. Schweiger, *J. Magn. Reson.*, 2006, **178(1)**, 42-55.

Crystallographic details

MSC#19051 $(Bpin)_2$Bpy (3)

CCDC: 1951270

Single crystals suitable for X-ray diffraction analysis were grown by slow evaporation of a concentrated solution of **3** in acetonitrile. A yellow crystal (approximate dimensions 0.25 × 0.23 × 0.12 mm3) was placed onto the tip of a MiTeGen pin and mounted on a Bruker Kappa Duo diffractometer equipped with an ApexII CCD detector at 293 K.

Data collection

The data collection was carried out using Mo Kα radiation (λ = 0.71073 Å, graphite monochromator) with a frame time of 10 seconds and a detector distance of 60 mm. A collection strategy was calculated and complete data to a resolution of 0.77 Å with a redundancy of 4 were collected. Six major sections of frames were collected with 0.50º ω and ϕ scans. The total exposure time was 7.48 hours. The frames were integrated with the Bruker SAINT[1] software package using a narrow-frame algorithm. The integration of the data using a monoclinic unit cell yielded a total of 22487 reflections to a maximum θ angle of 27.49° (0.77 Å resolution). The final cell constants of a = 6.5143(6) Å, b = 10.6792(9) Å, c = 16.5422(14) Å, β = 98.808(5)°, volume = 1137.23(17) $Å^3$, are based upon the refinement of the XYZ-centroids of 7792 reflections above 20 σ(I) with 6.277° < 2θ < 48.60°. Data were corrected for absorption effects using the Multi-Scan method (SADABS).[2] The ratio of minimum to maximum apparent transmission was 0.878. Table S1 contains additional crystal and refinement information.

Structure solution and refinement

The space group P 2_1/n was determined based on intensity statistics and systematic absences. The structure was solved using XS (Sheldrick, 2008)[3] and refined using full-matrix least-squares on F^2 within the Olex2 suite. 4 A direct-methods solution was calculated, which provided most nonhydrogen atoms from the E-map. Full-matrix least squares / difference Fourier cycles were performed, which located the remaining non-hydrogen atoms. All non-hydrogen atoms were refined with anisotropic displacement parameters. The hydrogen atoms were placed in ideal positions and refined as riding atoms with relative isotropic displacement parameters. The final full matrix least squares refinement converged to R1 = 0.0550 and wR2 = 0.1765 (F2, all data). The goodness-of-fit was 1.016. On the basis of the final model, the calculated density was 1.198 g/cm3 and F(000), 440 e- .

Twinning

The structure is non-merohedrally twinned. Two major and one minor domain could be identified and indexed.[5] In the refinement only two components were considered, with a domain ratio of 56:44. The twin element is 180 degree rotation about 0 0 1 in reciprocal space, twin law by the rows**:** 1 0 0, 0 -1 0, -0.791 0 -1.

MSC#19088 (DIM)Fe(NO_3)$_2$(MeCN) (4)

Single crystals suitable for X-ray diffraction analysis were grown by solvent diffusion of ether into a concentrated solution of **4** in acetonitrile. A red crystal (approximate dimensions 0.42 × 0.17 × 0.12 mm3) was placed onto the tip of a MiTeGen pin and mounted on a Bruker Kappa Duo diffractometer equipped with an ApexII CCD detector at 173.0 K.

CCDC: 1951269

Data Collection

The data collection was carried out using Mo Kα radiation (λ = 0.71073 Å, graphite monochromator) with a frame time of 0.5 seconds and a detector distance of 40 mm. A collection strategy was calculated and complete data to a resolution of 0.84 Å with a redundancy of 4 were collected. Four major sections of frames were collected with 0.50º ω and ϕ scans. The total exposure time was 34.20 hours. The frames were integrated with the Bruker SAINT[1] software package using a narrow-frame algorithm. The integration of the data using an orthorhombic unit cell yielded a total of 41333 reflections to a maximum θ angle of 25.05° (0.84 Å resolution). The final cell constants of a = 11.6059(10) Å, b = 15.9471(13) Å, c =

17.0224(11) Å, volume = 3150.5(6) Å^3, are based upon the refinement of the XYZ-centroids of 9962 reflections above 20 σ(I) with 4.956° < 2θ < 50.09°. Data were corrected for absorption effects using the Multi-Scan method (SADABS).[2] The ratio of minimum to maximum apparent transmission was 0.922.Table S2 contains additional crystal and refinement information.

Structure solution and refinement

The space group $Pca2_1$ was determined based on intensity statistics and systematic absences. The structure was solved using XT[3] and refined using full-matrix least-squares on F^2 within the OLEX2 suite.[4] An intrinsic phasing solution was calculated, which provided most non-hydrogen atoms from the E-map. Full-matrix least squares / difference Fourier cycles were performed, which located the remaining non-hydrogen atoms. All non-hydrogen atoms were refined with anisotropic displacement parameters. The hydrogen atoms were placed in ideal positions and refined as riding atoms with relative isotropic displacement parameters. The final full matrix least squares refinement converged to R1 = 0.0263 and wR2 = 0.0664 (F^2, all data). The goodness-of-fit was 1.044. On the basis of the final model, the calculated density was 1.313 g/cm3 and F(000), 1312 e- . The remaining electron density is minuscule.

MSC#19087 (DIM)Fe(NO)$_2$ (5)

CCDC: 1951267

Single crystals suitable for X-ray diffraction analysis were grown by slow diffusion of pentane into a concentrated solution of **5** in THF. An orange crystal (approximate dimensions 0.57 × 0.18 × 0.08 mm3) was placed onto the tip of a MiTeGen pin and mounted on a Bruker Kappa Duo diffractometer equipped with an ApexII CCD detector at 173 K.

Data Collection

The data collection was carried out using Mo Kα radiation (λ = 0.71073 Å, graphite monochromator) with a frame time of 90 seconds and a detector distance of 40 mm. A collection strategy was calculated and complete data to a resolution of 0.84 Å with a redundancy of 3.5 were collected. The total exposure time was 17.03 hours. The frames were integrated with the Bruker SAINT[1] software package using a narrow-frame algorithm. The integration of the data using an orthorhombic unit cell yielded a total of 30859 reflections to a maximum θ angle of 25.10° (0.84 Å resolution). The final cell constants of a = 14.0826(9) Å, b = 17.5521(15) Å, c = 18.3081(17) Å, volume = 4525.4(10) Å^3, are based upon the refinement of the XYZ-centroids of 2638 reflections above 20 σ(I) with 4.449° < 2θ < 45.61°. Data were corrected for absorption effects using the Multi-Scan method (SADABS).[2] The ratio of minimum to maximum apparent transmission was 0.890. Table S3 contains additional crystal and refinement information.

Structure solution and refinement

The space group Pbca was determined based on intensity statistics and systematic absences. The structure was solved using XT[3] and refined using full-matrix least-squares on F^2 within the OLEX2 suite.[4] An intrinsic phasing solution was calculated, which provided most non-hydrogen atoms from the E-map. Full-matrix least squares / difference Fourier cycles were performed, which located the remaining non-hydrogen atoms. All non-hydrogen atoms were refined with anisotropic displacement parameters. The hydrogen atoms were placed in ideal positions and refined as riding atoms with relative isotropic displacement parameters. The final full matrix least squares refinement converged to R1 = 0.0462 and wR2 = 0.0987 (F2, all data). The goodness-of-fit was 1.005. On the basis of the final model, the calculated density was 1.281 g/cm3 and F(000), 1840 e- . The remaining electron density is minuscule and mainly located around the iron center.

Table S1. Crystal data and structure refinement for 19051.

Empirical formula	C11 H16 B N O2	
Formula weight	205.06	
Crystal color, shape, size	yellow block, 0.25 × 0.23 × 0.12 mm^3	
Temperature	293 K	
Wavelength	0.71073 Å	
Crystal system, space group	Monoclinic, P 1 21/n 1	
Unit cell dimensions	a = 6.5143(6) Å	⍰ = 90°.
	b = 10.6792(9) Å	⍰ = 98.808(5)°.
	c = 16.5422(14) Å	⍰ = 90°.
Volume	1137.23(17) $Å^3$	
Z	4	
Density (calculated)	1.198 g/cm^3	
Absorption coefficient	0.080 mm^{-1}	
F(000)	440	

Data collection

Diffractometer	Kappa Apex II Duo, Bruker
Theta range for data collection	2.278 to 27.493°.
Index ranges	-8<=h<=8, 0<=k<=13, 0<=l<=21
Reflections collected	22487
Independent reflections	4619 [Rint = 0.0372]
Observed Reflections	2692
Completeness to theta = 25.242°	100.0 %

Solution and Refinement

Absorption correction	Semi-empirical from equivalents
Max. and min. transmission	1 and 0.88
Solution	Intrinsic methods
Refinement method	Full-matrix least-squares on F^2
Weighting scheme	w = [⍰^{2}Fo^2+ AP^2+ BP]$^{-1}$, with P = (Fo^2+ 2 Fc^2)/3, A = , B =
Data / restraints / parameters	4619 / 0 / 141
Goodness-of-fit on F^2	1.016
Final R indices [I>2⍰(I)]	R1 = 0.0550, wR2 = 0.1410
R indices (all data)	R1 = 0.1102, wR2 = 0.1765

Extinction coefficient	n/a
Largest diff. peak and hole	0.162 and -0.206 e.Å^{-3}

Twin Details

Type, twin law	non-merohedral, 1 0 0, 0 -1 0, -0.791 0 -1
Twin element, domain ratio	180° rotation in reciprocal space about 1 0 0, 55.9 : 44.1

Table S2. Crystal data and structure refinement for 19088.

Empirical formula	C28 H37 Fe N7 O6	
Formula weight	623.49	
Crystal color, shape, size	red plate, 0.42 × 0.17 × 0.12 mm^3	
Temperature	173.0 K	
Wavelength	0.71073 Å	
Crystal system, space group	Orthorhombic, $Pca2_1$	
Unit cell dimensions	a = 17.0228(4) Å	? = 90°.
	b = 11.6142(4) Å	? = 90°.
	c = 15.9579(5) Å	? = 90°.
Volume	3154.98(16) Å^3	
Z	4	
Density (calculated)	1.313 g/cm^3	
Absorption coefficient	0.528 mm^{-1}	
F(000)	1312	

Data collection

Diffractometer	Kappa Apex II Duo, Bruker
Theta range for data collection	2.123 to 25.078°.
Index ranges	-20<=h<=20, -13<=k<=13, -19<=l<=19
Reflections collected	38729
Independent reflections	5587 [Rint = 0.0408]
Observed Reflections	5084
Completeness to theta = 25.078°	99.9 %

Solution and Refinement

Absorption correction	Semi-empirical from equivalents
Max. and min. transmission	0.7452 and 0.6873
Solution	Intrinsic methods
Refinement method	Full-matrix least-squares on F^2
Weighting scheme	w = [?^{2}Fo^2+ AP^2+ BP]$^{-1}$, with
	P = (Fo^2+ 2 Fc^2)/3, A = , B =
Data / restraints / parameters	5587 / 349 / 390
Goodness-of-fit on F^2	1.044

Final R indices [I>2⍰(I)]	R1 = 0.0263, wR2 = 0.0643
R indices (all data)	R1 = 0.0323, wR2 = 0.0664
Absolute structure parameter	0.007(5)
Extinction coefficient	n/a
Largest diff. peak and hole	0.196 and -0.179 e.Å^{-3}

Table S3. Crystal data and structure refinement for 19087.

Empirical formula	C22 H28 Fe N4 O2	
Formula weight	436.33	
Crystal color, shape, size	orange plate, 0.57 × 0.18 × 0.08 mm^3	
Temperature	173 K	
Wavelength	0.71073 Å	
Crystal system, space group	Orthorhombic, Pbca	
Unit cell dimensions	a = 17.5520(15) Å	⍰ = 90°.
	b = 14.0826(9) Å	⍰ = 90°.
	c = 18.3080(17) Å	⍰ = 90°.
Volume	4525.3(6) Å^3	
Z	8	
Density (calculated)	1.281 g/cm^3	
Absorption coefficient	0.690 mm^{-1}	
F(000)	1840	

Data collection

Diffractometer	Kappa Apex II Duo, Bruker
Theta range for data collection	2.162 to 25.061°.
Index ranges	-20<=h<=20, -12<=k<=16, -21<=l<=21
Reflections collected	28523
Independent reflections	4007 [Rint = 0.1110]
Observed Reflections	2493
Completeness to theta = 25.061°	99.8 %

Solution and Refinement

Absorption correction	Semi-empirical from equivalents
Max. and min. transmission	0.7452 and 0.6632
Solution	Intrinsic methods
Refinement method	Full-matrix least-squares on F^2
Weighting scheme	w = [⍰^{2}Fo^2+ AP^2+ BP]$^{-1}$, with
	P = (Fo^2+ 2 Fc^2)/3, A = , B =
Data / restraints / parameters	4007 / 0 / 270
Goodness-of-fit on F^2	1.005
Final R indices [I>2⍰(I)]	R1 = 0.0462, wR2 = 0.0832

R indices (all data)	R1 = 0.0986, wR2 = 0.0987
Extinction coefficient	n/a
Largest diff. peak and hole	0.272 and -0.290 e.Å^{-3}

1 SAINT, Bruker Analytical X-Ray Systems, Madison, WI, current version.

2 SADABS, Bruker Analytical X-Ray Systems, Madison, WI, current version.

3 G. M. Sheldrick, *Acta Cryst*., 2008, **A64**, 112 - 122. G. M. Sheldrick, *Acta Cryst,* 2015, **A71**, 3-8

4 O. V. Dolomanov, L. J. Bourhis, R. J. Gildea, J. A. K. Howard and H. Puschmann, *J. Appl. Crystallogr.*, 2009, **42**, 339–341

5 G. M. Sheldrick, CELL NOW, University of Göttingen, Germany, (2018).

Computational Details

DFT[1] calculations were carried out using Gaussian 16[2]. Geometry optimizations were performed at the B3LYP/6-31G(d,p) level of theory[3] for organic molecules, and TPSSH/def2TZVP[4,5] level of theory for all iron containing species. All optimized structures were confirmed to be minima by analyzing the harmonic frequencies.[6-8] Cartesian Coordinates are summarized in Table S1.

1. Parr, R.G.; Yang, W. Density-functional theory of atoms and molecules; Oxford University Press: New York, 1989.
2. Gaussian 16, Revision B.01, M. J. Frisch, G. W. Trucks, H. B. Schlegel, G. E. Scuseria, M. A. Robb, J. R. Cheeseman, G. Scalmani, V. Barone, G. A. Petersson, H. Nakatsuji, X. Li, M. Caricato, A. V. Marenich, J. Bloino, B. G. Janesko, R. Gomperts, B. Mennucci, H. P. Hratchian, J. V. Ortiz, A. F. Izmaylov, J. L. Sonnenberg, D. Williams-Young, F. Ding, F. Lipparini, F. Egidi, J. Goings, B. Peng, A. Petrone, T. Henderson, D. Ranasinghe, V. G. Zakrzewski, J. Gao, N. Rega, G. Zheng, W. Liang, M. Hada, M. Ehara, K. Toyota, R. Fukuda, J. Hasegawa, M. Ishida, T. Nakajima, Y. Honda, O. Kitao, H. Nakai, T. Vreven, K. Throssell, J. A. Montgomery, Jr., J. E. Peralta, F. Ogliaro, M. J. Bearpark, J. J. Heyd, E. N. Brothers, K. N. Kudin, V. N. Staroverov, T. A. Keith, R. Kobayashi, J. Normand, K. Raghavachari, A. P. Rendell, J. C. Burant, S. S. Iyengar, J. Tomasi, M. Cossi, J. M. Millam, M. Klene, C. Adamo, R. Cammi, J. W. Ochterski, R. L. Martin, K. Morokuma, O. Farkas, J. B. Foresman, and D. J. Fox, Gaussian, Inc., Wallingford CT, 2016.
3. (a) Vosko, S. H.; Wilk, L.; Nusair, M. *Can. J. Phys*. 1980, **58**, 1200. (b) Lee, C.; Yang, W.; Parr, R.G. Phys. Rev. B 1988, **37**, 785. (c) Becke, A. D. *J. Chem. Phys*. 1993, **98**, 5648. (d) Stephens, P.J.; Devlin, F. J.; Chabalowski, C. F.; Frisch, M.J. *J. Phys. Chem*. 1994, **98**, 11623
4. Staroverov, V. N.; Scuseria, G. E.; Tao. J.; Perdew, J. P. *J. Chem. Phys*. 2003, **91**, 146401.
5. Schäfer, A.; Huber, C.; Ahlrichs, R. *J. Chem. Phys*. 1994, **100**, 5829-5835.
6. Becke, A.D. *J. Chem. Phys*., 1993, **98**, 1372.
7. (a) Schlegel, H. B.; McDouall, J. J. in Computational Advances in Organic Chemistry; Oeretir, C; Csizmadia, I. G., Eds.; Kluwer Academic: Amsterdam, The Netherlands, 1991. (b) Bauernschmitt, R.; Ahlrichs, R. *J. Chem. Phys*. 1996, **104**, 9047.
8. Schlegel, H. B. *WIREs Comput. Mol. Sci*. 2011, **1**, 790.

Corresponding orbital analysis

The unrestricted corresponding orbital diagram in Figure S16 of $[DIMFe(NO)_2]^+$ shows much delocalization of the paired electrons across the $Fe(NO)_2$ fragment, supporting the assignment of antiferromagnetic coupling between iron unpaired electrons and nitrosyl unpaired electrons. Interestingly, the singly occupied alpha electron appears to lie in a d orbital with minimal delocalization. However, when the isovalue is decreased (Figure S17), the orbital shows character on the nitrosyl ligands as well as the DIM ligands, which is supported by the spin density plot, as well as the experimental EPR data.

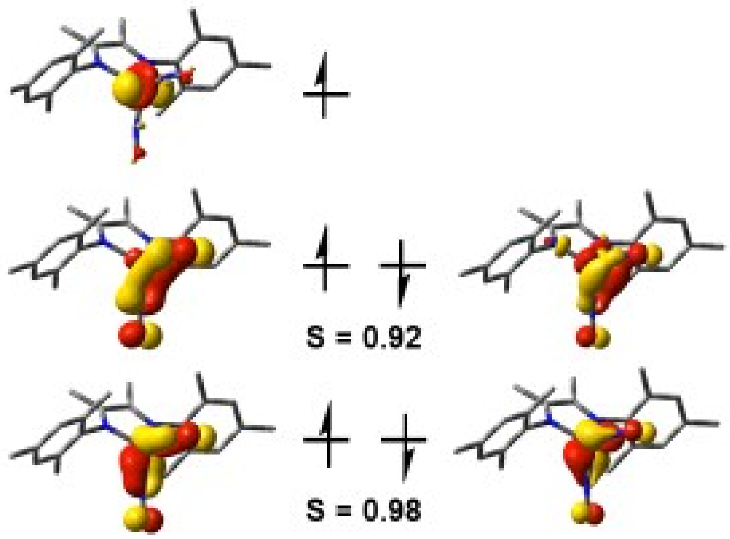

Figure S18. Corresponding orbital diagram for $[(DIM)Fe(NO)_2]^+$ (isovalue 0.05 au)

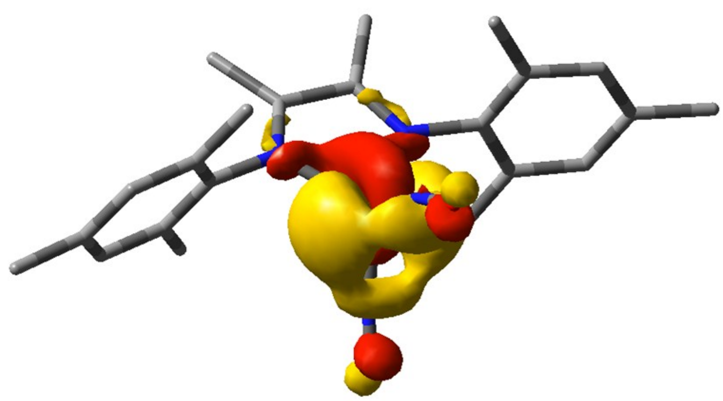

Figure S19. Unpaired alpha spin from Figure S16 plotted at an isovalue of 0.025 au

DIMFe(κ²-ON=NO) analysis

Geometry optimization of S = 2 (DIM)Fe(ONNO), starting from a tetrahedral structure, yielded a planar structure (Figure S18). This shows normal N=C-C=N distances within DIM and distances consistent with a dianionic $[O\text{-}N{=}N\text{-}O]^{2-}$ hyponitrite bonding.

Calculated distances match well the values, typically N=N 1.24 Å and N-O 1.37 Å, found among 5 structure determinations (KIRPUZ, XOCYEW, MEHQAT, MORSUH, VIKQAI) of coordinated hyponitrite.

While S = 2 would appear to be an unfavorable spin state for a planar structure, it has been shown, by both experiment and DFT energy calculations of this structural change,[1] that the energy penalty for being planar can be overcome by strongly π donating ligands, together with steric preferences for an angle X-Fe-X of 90° vs. 109°. This modest energy penalty is also presumably why a tetradentate ligand can yield planar Fe(II) as the lowest energy structure.

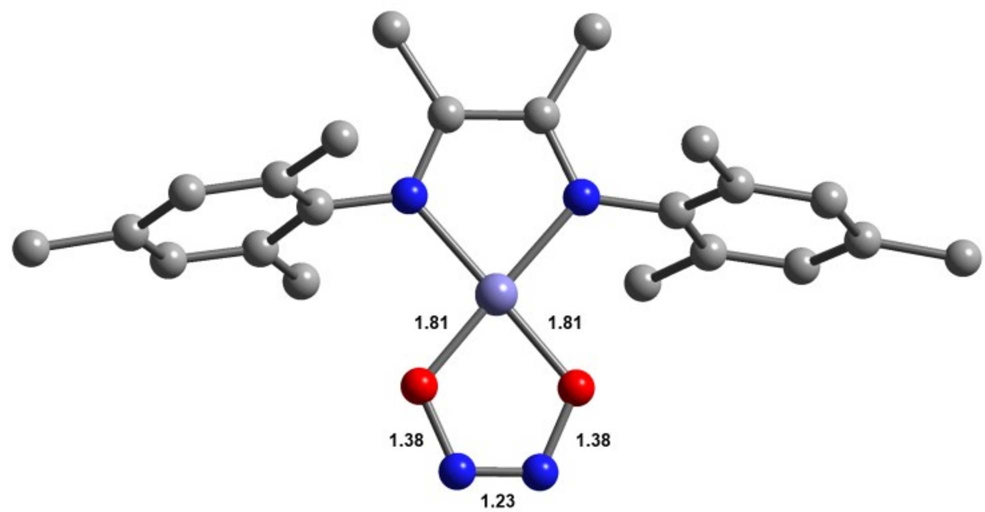

Figure S20. Optimized structure for S = 2 (DIM)Fe(ONNO)

1. X. Wurzenberger, H. Piotrowski, P. Kluefers, Angew. *Chem. Int. Ed.*, 2011, **50**, 4974-4978.

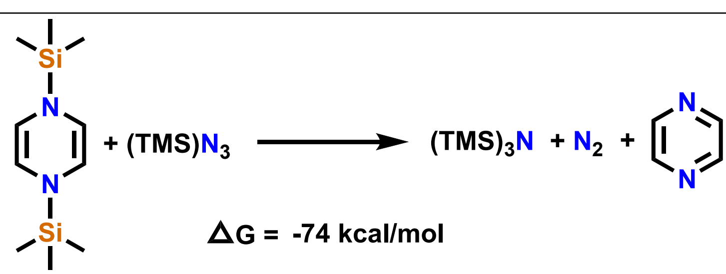

Scheme S1. Computed thermodynamics for the silylation of trimethylsilyl azide using $(TMS)_2$Pz **2**

Reaction	ΔG°	ΔG°	ΔG°

	kcal/mol	$(TMS)_2Pz$ Derivative	$(Bpin)_2bpy$ derivative
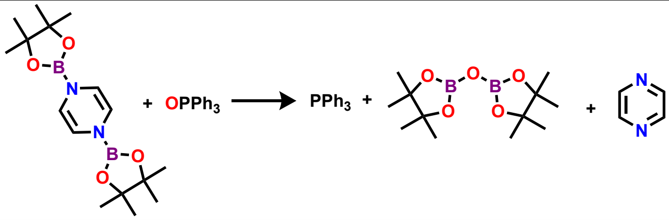	-24.6	-50.4	-33.7
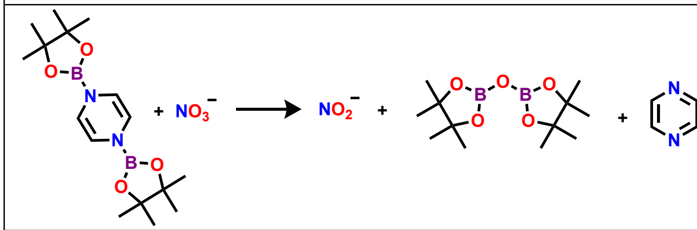	-47.8	-73.1	-56.9
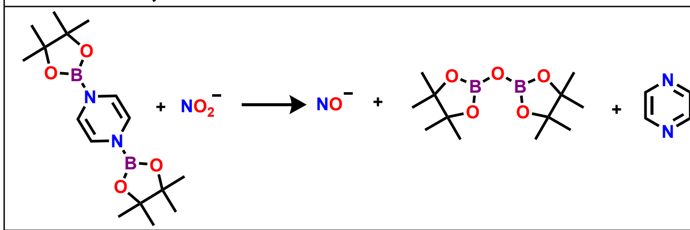	-21.4	-47.2	-30.5
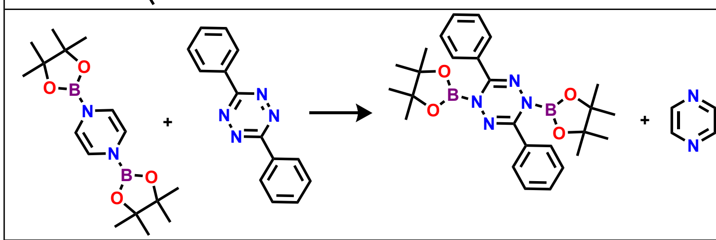	-9.4	-29.3	-18.5
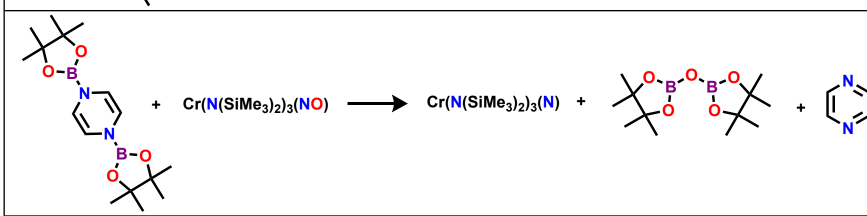	-52.3	-76.6	-61.4

Table S4. Thermodynamics for reductive transformations using $(Bpin)_2Pz$, and comparisons to $(TMS)_2Pz$ as well as $(Bpin)_2Bpy$. The value for NO^- is for triplet product, and singlet is calculated to be 10 kcal/mol less stable. The absolute energy of anions will certainly be influenced by cations, but we evaluate the free anion thermodynamics for the *trends* that they convey.

To gain insight into the potential reactivity of $(Bpin)_2Pz$, computations were done at the B3LYP/6-31G(d,p) level of theory on reductive borylations that had been previously calculated for $(TMS)_2Pz$. While overall reagent effectiveness hinges on mechanism, knowing thermodynamics is fundamental. The calculated geometry of $(Bpin)_2Pz$ is planar with BO_2 eclipsing the planar nitrogen rings; BO and BN distances, 1.38 and 1.42 Å, respectively, both indicate pi bonding. The same is true for $(Bpin)_2bpy$. Distances agree well with experiment.

We addressed the questions of whether the boron reagent is more or less powerful for deoxygenation, and also whether the 4,4' bpy boron reagent is more or less powerful then the single ring (pyrazine) version. The reaction free energies for borylation of diphenyl tetrazine is favorable, as is deoxygenation of nitrate. The 4,4'-bipyridine reagent, $(Bpin)_2Bpy$, is uniformly more powerful than $(Bpin)_2Pz$ by ~ 9 kcal/mol, which is consistent with Mashima's and Suginome's experimental observations. The pyrazine-based data show that silylation is uniformly more exergonic than borylation by 20 - 26 kcal/mol. The constancy of these shifts over change from complexed (see chromium nitrosyl example in Table) to free substrate, and involving transfer between nitrogens in different heterocycles, is remarkable; they certainly show Si is more potent than B, and that the bpy transfer reagent is more potent than the pyrazine analog. Furthermore, perhaps the very favorable thermodynamics of $(TMS)_2Pz$ has contributed to selectivity issues with deoxygenation of our compounds, and the "milder" $(Bpin)_2Pz$ may lead to enhanced selectivity. Both reduction of nitrate to nitrite, then nitrite to NO^-, are thermodynamically favorable for each reagent, consistent with our expectations for pentavalent and trivalent nitrogen being good oxidizing agents. Deoxygenation of nitrate is more exothermic than nitrite by 26 kcal/mol. Independent of reagent, oxidants ranked according to decreasing exergonic character are CrNO > NO_3^- > $OPPh_3$ > NO_2^-> Ph_2Tz.

Table S5. Cartesian coordinated (in Å) for all optimized species.

[(DIM)Fe(NO)$_2$]$^+$

Fe	-0.000083	-0.484814	-0.880121
N	0.256686	-2.191169	-0.994137
N	1.296044	0.374468	0.455137
O	0.401821	-3.286009	-1.356535
N	-1.295791	0.177043	0.564002
C	-2.712989	0.106679	0.368707
N	-0.258273	0.342839	-2.376476
C	2.713425	0.251964	0.287988
C	5.446442	-0.054028	-0.162856
C	-0.750613	0.819147	1.538626
O	-0.405938	0.631059	-3.492738
C	0.751630	0.849598	1.521474
C	-3.387336	1.210905	-0.170310
C	-5.445357	-0.100765	-0.140043
C	3.391000	-0.799788	0.921459
C	-3.366025	-1.104044	0.650389
C	-4.732701	-1.175899	0.399498
C	-4.753652	1.076611	-0.420141
C	3.363559	1.149436	-0.572705
C	4.756914	-0.932080	0.673450
C	4.731638	0.981868	-0.769672
H	-5.288349	1.918687	-0.845602
H	-5.256041	-2.097407	0.630866
H	5.294494	-1.744765	1.149721
H	5.253197	1.680143	-1.415163
C	-2.618598	-2.278446	1.226932
H	-1.910369	-2.698572	0.507202
H	-2.046295	-2.000484	2.116001
H	-3.309746	-3.072094	1.508687
C	-6.918353	-0.227135	-0.426009
H	-7.092962	-0.909102	-1.263569
H	-7.453829	-0.629453	0.437282
H	-7.359794	0.736571	-0.681958
C	-2.672379	2.500111	-0.485132
H	-2.554779	3.123415	0.407427
H	-1.675969	2.323539	-0.895783
H	-3.236743	3.083184	-1.212403
C	-1.500981	1.494767	2.637139
H	-1.347855	2.577429	2.592544
H	-2.566515	1.288523	2.563921
H	-1.133456	1.160850	3.610474
C	1.503101	1.411674	2.681500
H	1.348079	0.793142	3.570845
H	2.568780	1.458113	2.468366
H	1.138015	2.413039	2.922322
C	2.677546	-1.765192	1.833229
H	2.548362	-1.349492	2.837969
H	1.686065	-2.024280	1.455652
H	3.248800	-2.687229	1.937411
C	2.613788	2.272438	-1.241198
H	1.895865	1.897054	-1.975872
H	2.051636	2.872566	-0.520584
H	3.302159	2.935763	-1.763745
C	6.917120	-0.233694	-0.431576
H	7.072560	-0.795624	-1.358077
H	7.420500	0.728294	-0.544624
H	7.405543	-0.784072	0.373845

(DIM)Fe(NO)$_2$

Fe	0.005517	0.169341	0.929338
C	4.679816	-1.209027	0.175236
H	5.202000	-2.142412	0.360530
C	-2.628258	-0.067534	-0.302896
C	-3.316176	1.148940	-0.415592
C	2.556881	-2.550687	-0.115176
H	3.148012	-3.352743	0.327971
H	2.310490	-2.844976	-1.141288
H	1.615166	-2.466594	0.429843
C	5.390797	-0.009398	0.199715
C	1.528623	-0.453265	-2.979627
H	2.592773	-0.338405	-2.781320
H	1.235460	0.268495	-3.747623
H	1.359749	-1.451221	-3.397019
C	-2.585246	2.419177	-0.763174
H	-1.994226	2.312131	-1.676641
H	-1.891259	2.699271	0.032447
H	-3.288465	3.240089	-0.908342
C	-5.381185	-0.006517	0.175074
C	-2.533340	-2.549450	0.181326
H	-1.916469	-2.542612	1.083146
H	-1.860480	-2.722639	-0.661843
H	-3.223078	-3.391954	0.247517
C	3.324259	1.189409	-0.297823
C	-0.715413	-0.271417	-1.725524
C	0.728162	-0.255615	-1.729631
C	2.593256	2.485645	-0.530062
H	1.988787	2.755634	0.338967
H	1.910830	2.419929	-1.380615
H	3.299093	3.295908	-0.718154
C	2.643318	-0.035837	-0.311402
C	3.310389	-1.247369	-0.083529
C	-1.519033	-0.473828	-2.972891
H	-2.583264	-0.510256	-2.747632
H	-1.234801	-1.404882	-3.472201
H	-1.343749	0.338234	-3.685942
C	-3.289646	-1.254565	0.039802
C	4.695396	1.175287	-0.044881
H	5.232551	2.118506	-0.037409
C	-4.688650	1.154030	-0.171103
H	-5.229229	2.091430	-0.255832
C	-4.663733	-1.198510	0.272000
H	-5.184819	-2.113653	0.534902
N	-1.220690	-0.093435	-0.524960
N	1.236619	-0.053356	-0.534852
N	-0.037458	1.661220	1.573294
N	0.002730	-1.014234	2.049637
O	-0.083776	2.720074	2.087708
O	-0.039013	-1.789431	2.933844
C	-6.859808	0.033602	0.468691
H	-7.336617	-0.922595	0.242223
H	-7.042334	0.248854	1.526923
H	-7.360470	0.810165	-0.113951
C	6.865115	0.011046	0.516200
H	7.369300	0.837473	0.010195
H	7.032171	0.134496	1.591543
H	7.350179	-0.919752	0.214167

(Bpin)$_2$Pz

C	0.667404	1.170377	-0.245824
C	-0.667407	1.170388	-0.245764
C	-0.667404	-1.170400	0.245709
C	0.667406	-1.170411	0.245649
H	1.239129	2.068228	-0.433447
H	-1.239135	2.068248	-0.433337
H	-1.239130	-2.068253	0.433324
H	1.239134	-2.068273	0.433213
N	1.430152	-0.000023	-0.000118
N	-1.430153	0.000001	0.000009
B	2.844624	-0.000007	-0.000044
B	-2.844625	-0.000001	0.000005
O	3.599089	-1.115369	0.307080
O	3.599096	1.115367	-0.307108
O	-3.599093	1.115368	-0.307087
O	-3.599092	-1.115369	0.307100
C	-4.967875	-0.785334	-0.047638
C	-4.967871	0.785340	0.047668
C	-5.197435	1.295637	1.473370
H	-4.970766	2.364228	1.505881
H	-6.233382	1.150990	1.792442
H	-4.539866	0.786339	2.182892
C	-5.905180	1.487490	-0.926327
H	-6.944016	1.196747	-0.740554
H	-5.826903	2.570197	-0.796127
H	-5.654360	1.251981	-1.961382
C	-5.197459	-1.295630	-1.473337
H	-4.970792	-2.364222	-1.505851
H	-6.233410	-1.150981	-1.792395
H	-4.539898	-0.786332	-2.182866
C	-5.905173	-1.487481	0.926370
H	-6.944011	-1.196737	0.740611
H	-5.826901	-2.570189	0.796169
H	-5.654339	-1.251972	1.961421
C	4.967868	0.785342	0.047676
C	4.967878	-0.785332	-0.047627
C	5.197401	1.295642	1.473382
H	6.233341	1.151000	1.792476
H	4.970726	2.364233	1.505886
H	4.539818	0.786343	2.182890
C	5.905195	1.487493	-0.926302
H	5.826913	2.570200	-0.796105
H	6.944029	1.196754	-0.740506
H	5.654398	1.251981	-1.961361
C	5.905157	-1.487473	0.926404
H	5.826892	-2.570181	0.796204
H	6.943998	-1.196724	0.740668
H	5.654298	-1.251962	1.961449
C	5.197497	-1.295631	-1.473320
H	6.233454	-1.150977	-1.792356
H	4.970836	-2.364224	-1.505835
H	4.539949	-0.786340	-2.182866

(DIM)Fe(ONNO)

Fe	-0.000872	-0.838945	0.238080
N	1.283515	0.555242	-0.186421
N	-1.283788	0.551133	-0.204721
C	-2.548247	-1.050915	-2.178232
H	-1.950613	-0.322022	-2.732556
H	-1.859786	-1.787385	-1.753663

$(TMS)_2Pz$ 2

C	-0.772372	0.974216	-0.095371
C	0.551989	0.974246	0.091958
C	0.551941	3.341323	0.092024
C	-0.772425	3.341302	-0.095272
H	-1.304079	0.034329	-0.175008
H	1.083897	0.034366	0.170358
H	1.083804	4.281228	0.170505
H	-1.304171	4.281181	-0.174860
Si	3.094751	2.158155	0.058724
Si	-3.315118	2.158104	-0.058463
N	1.337646	2.157792	0.213495
N	-1.558243	2.157739	-0.215782
C	3.755171	0.608291	0.911276
H	3.463843	-0.312629	0.395479
H	4.850712	0.632646	0.928612
H	3.405712	0.540207	1.946405
C	3.655008	2.160745	-1.749463
H	3.279839	3.043988	-2.277903
H	4.748309	2.161620	-1.833549
H	3.281035	1.278420	-2.280272
C	3.754925	3.705978	0.915217
H	4.850467	3.681606	0.932856
H	3.463758	4.628145	0.401561
H	3.405101	3.771548	1.950384
C	-3.976673	0.607743	-0.909225
H	-3.684596	-0.312864	-0.393295
H	-5.072237	0.632071	-0.925021
H	-3.628701	0.539064	-1.944817
C	-3.872788	2.161675	1.750521
H	-3.496940	3.045257	2.277909
H	-4.965968	2.162504	1.836193
H	-3.497961	1.279693	2.281296
C	-3.976595	3.705452	-0.914817
H	-5.072165	3.681129	-0.930716
H	-3.684574	4.627892	-0.402133
H	-3.628398	3.770427	-1.950569

$(TMS)N_3$

Si	-0.665617	0.000075	0.019886
C	-0.759617	1.552969	1.082608
H	-0.685214	2.457532	0.470787
H	-1.709479	1.593822	1.627902
H	0.046737	1.581910	1.823390
C	-0.759253	-1.546447	1.091919
H	-1.709133	-1.584227	1.637408
H	-0.684642	-2.454647	0.485538
H	0.047073	-1.570740	1.832893
C	-1.962843	-0.004226	-1.334389
H	-1.864384	0.878159	-1.974290
H	-1.864350	-0.890655	-1.968680
H	-2.973159	-0.002919	-0.911129
N	0.881815	-0.002337	-0.869500
N	1.993250	-0.000983	-0.355375
N	3.068573	0.000026	0.033011

N(TMS)$_3$

N	-0.011153	0.006565	-0.039840
Si	1.141826	1.362373	0.018643
Si	0.622561	-1.658780	-0.018752
Si	-1.766407	0.297845	-0.020297
C	-0.711929	-2.992661	0.190884
H	-1.548279	-2.925205	-0.509508
H	-0.221101	-3.957191	0.012158
H	-1.117678	-3.023556	1.205060
C	1.497399	-2.087754	-1.643804
H	2.388392	-1.485924	-1.834943
H	1.803662	-3.140341	-1.637261
H	0.814912	-1.948898	-2.489605
C	1.776812	-1.939473	1.461160
H	1.224178	-1.803950	2.397593
H	2.149690	-2.970525	1.448293
H	2.645875	-1.278331	1.494195
C	-2.620675	-0.505314	1.471722
H	-3.635311	-0.099644	1.561399
H	-2.710429	-1.590741	1.404105
H	-2.091922	-0.269007	2.401758
C	-2.567317	-0.307893	-1.627575
H	-3.650891	-0.142876	-1.600354
H	-2.170377	0.248253	-2.484179
H	-2.401446	-1.371284	-1.822708
C	-2.229913	2.132833	0.115748
H	-2.050256	2.691953	-0.805079
H	-3.307675	2.171946	0.313333
H	-1.736267	2.658614	0.938361
C	0.707714	2.777785	-1.169179
H	-0.004911	3.495909	-0.759326
H	1.629428	3.326208	-1.395831
H	0.310300	2.406778	-2.119801
C	1.265753	2.038434	1.783155
H	1.634535	1.269667	2.470652
H	1.955159	2.889355	1.832493
H	0.295540	2.376023	2.161920
C	2.895816	0.876919	-0.527423
H	3.335119	0.016532	-0.019725
H	2.941842	0.694465	-1.605651
H	3.542298	1.738425	-0.320910

N$_2$

N	0.000000	0.000000	0.546000
N	0.000000	0.000000	-0.546000

Pyrazine

C	1.133718	-0.698186	0.000025
C	1.133724	0.698176	0.000037
N	0.000004	1.408894	0.000015
C	-1.133715	0.698190	-0.000024
C	-1.133721	-0.698180	-0.000038
N	-0.000009	-1.408894	-0.000014
H	2.067983	-1.255573	0.000052
H	2.067994	1.255556	0.000076
H	-2.067985	1.255570	-0.000049
H	-2.067997	-1.255551	-0.000079